

**Supplemental Information:**  
**Segmentation of dense and multi-species bacterial colonies using  
models trained on synthetic microscopy images**

Vincent Hickl,\* Abid Khan, René M. Rossi,  
Bruno F. B. Silva, and Katharina Maniura-Weber

---

\* Email address; [vincent.hickl@empa.ch](mailto:vincent.hickl@empa.ch)

## CONTENTS

S1. Synthetic image generation	S3
A. Rod-shaped cells and cell alignment	S3
B. Circular cells	S5
C. Clustering	S6
S2. Segmentation Model Training Parameters	S7
S3. CycleGAN training	S8
References	S9

## S1. SYNTHETIC IMAGE GENERATION

The raw (unprocessed) synthetic images of bacteria were binary images produced using custom Python functions. All code is publicly available as described in the main text.

In short, we begin by specifying the dimensions of the images, and generating an array filled with zeros that serves as a “canvas” on which to draw cells. Here, the canvas was chosen to be  $2048 \times 2048$  pixels in size, but synthetic images are later split into smaller images for processing and training. Then, for each cell to be drawn, the program determines the set of pixels that should be set to one to draw cells of the desired shape, size, and orientation on the canvas. Before drawing each cell, the algorithm checks how much this set of pixels overlaps with other cells to avoid excessive overlap. Cells with overlap above a chosen threshold are not drawn. Additionally, an option may be chosen to draw cells only in clusters, in which case cells are only drawn if they are within a predefined distance of previously drawn cells. In general, cell positions, dimensions, and orientations are chosen randomly from empirically determined distributions. Optionally, for rod-shaped cells, the orientation of each cell may instead be chosen to be the same as its nearest neighbor to simulate the alignment commonly observed in bacterial monolayers. In this case, a noise parameter is also introduced so the alignment is not exact, adding some fluctuations to the cell alignment. By combining these parameters and options in different ways, a diverse set of images can easily be produced to ensure the resulting segmentation algorithm is well-suited to study real experimental images.

Along with the binary image of bright cells on a dark background (which can be inverted to produce brightfield synthetic images), the algorithm produces a mask containing unique integer labels for each cell to be used for training of the segmentation algorithm.

Below, additional details of the methods for drawing each cell type and for the different methods within the algorithm are provided.

### A. Rod-shaped cells and cell alignment

*Pseudomonas aeruginosa* are modeled as rectangles of width  $w$  and length  $l$  with hemispherical caps of radius  $w/2$ . Thus, the actual length of each cell is  $l + w$ . The orientation of the cell is given by the angle  $\theta$ , measured with respect to the vertical, as shown in Fig. S1.

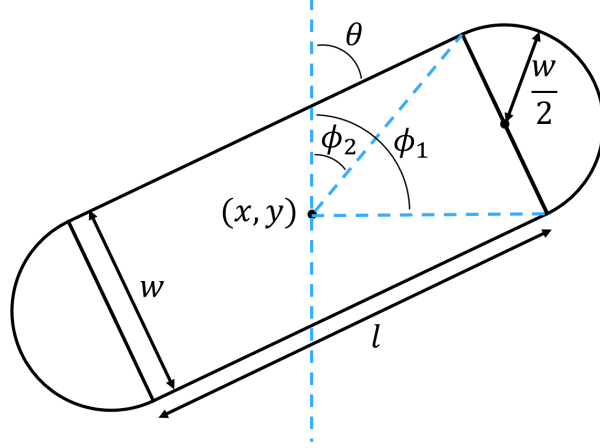


FIG. S1. Diagram of model rod-shaped cell.

First, the coordinates of the vertices of the rectangle are determined:

$$c = \{x + d \sin \phi_1, x + d \sin \phi_2, x - d \sin \phi_1, x - d \sin \phi_2\} \quad (1)$$

$$r = \{y + d \cos \phi_1, y + d \cos \phi_2, y - d \cos \phi_1, y - d \cos \phi_2\} \quad (2)$$

where,  $c$  and  $r$  refer to the columns and rows of the image array,  $(x, y)$  is the center of the cell (its location),  $d = \frac{1}{2}(w^2 + l^2)^{1/2}$  is half the size of the rectangle's diagonal, and the angles  $\phi_1 = \theta + \tan^{-1}(w/l)$  and  $\phi_2 = \theta - \tan^{-1}(w/l)$  are the angles between the center of the rectangle and the vertices. The endcaps are then simply drawn as circles with radius  $w/2$  centered on the short sides of the rectangle. The `draw.polygon` and `draw.ellipse` from the `scikit-image` library in Python are then used to obtain the set of pixels for each cell.

The lengths and widths of the rods are randomly drawn from distributions determined empirically by manually measuring the dimensions of 30-50 randomly chosen cells in the real microscopy images to be analyzed. We found that cell widths follow a normal distribution with a mean of  $\bar{w} = 0.8 \mu\text{m}$  and a standard deviation of  $\sigma_w = 0.1 \mu\text{m}$ . Cell lengths follow a normal distribution with  $\bar{l} = 2.7$  and  $\sigma_l = 0.6$ . In practice, we believe it is beneficial to increase the standard deviation slightly when generating synthetic images to ensure the segmentation algorithm can accurately produce masks for a variety of real cells. Further testing is required to determine which parameters lead to optimal segmentation results.

Once the set of pixels corresponding to the cell is found, the algorithm checks how many of these pixels are already 1. The amount of overlap permitted between cells can be chosen via

the parameter `thresh`, which is the maximum number of overlapping pixels above which the new cell is not drawn. The default value chosen here is `thresh = 5`, but this depends heavily on the magnification, camera, and experimental conditions used to capture a particular image.

If the number of overlapping pixels exceeds the threshold, the algorithm automatically rotates the cell from  $\theta$  to  $\theta + \pi$  in increments of 0.1, checking at each step whether the cell can now be drawn. This process reduces the number of cells that are not drawn because of excessive overlap, and introduced a small amount of cell alignment even when orientations are initially chosen randomly. If the cell cannot be drawn after all orientations have been tried, it is simply discarded and the algorithm moves on to the next set of coordinates and dimensions. This approach of removing cells that don't fit in a space introduces a slight bias towards smaller cells, but our results do not suggest that this prevents the segmentation model from accurately detecting large cells, nor does it lead to oversegmentation of rod-shaped cells (see Fig. 2 in the main text).

To simulate the tendency of rod-shaped cells to align, an option may be chosen to set each cell's orientation to  $\theta_j + \epsilon$ , where  $\theta_j$  is the orientation of the cell's nearest neighbor and  $\epsilon$  is a small random noise parameter to introduce fluctuations in the alignment. In this work  $\epsilon$  is chosen from a normal distribution with mean 0 and standard deviation 0.1 radians. The standard deviation can be set to vary the degree of cell alignment across different images. To generate images of aligned cells, a small number (usually 10-20) of randomly positioned and oriented cells is first generated, before the remainder of the cells is generated to be aligned with their neighbors. To efficiently find the cells' nearest neighbors, a K-D tree was created from the set of cell coordinates using the existing methods in the SciPy library for Python. This K-D tree is a data structure which can be queried to efficiently find nearest neighbors and distances between cell pairs.

## B. Circular cells

*Staphylococcus aureus* are modeled as circles of radius  $r$ . Their positions and dimensions are randomly chosen as for the rod-shaped cells above. Cell radii were manually measured and found to follow a normal distribution with a mean radius of  $\bar{r} = 0.65 \mu\text{m}$  and a standard deviation of  $\sigma_r = 0.10$ . It is common for *S. aureus* to remain tightly clustered after dividing,

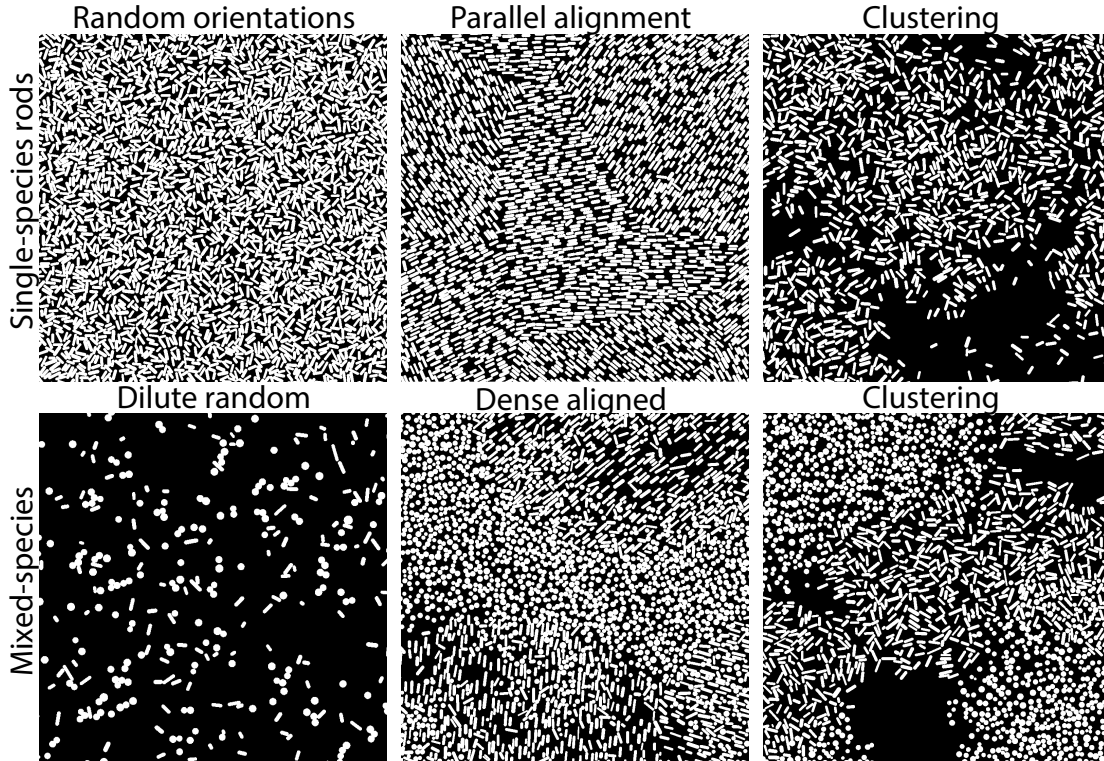


FIG. S2. Sample raw synthetic images, showing different arrangements of cells produces via different input parameters.

so to mimick this behavior and produce more realistic synthetic images a higher overlap threshold of 0.15 was chosen compared to the rod-shaped cells.

### C. Clustering

For both cell types, it is possible with our algorithm to produce images where cells tend to cluster together, meaning there are distinct regions of densely packed cells and more dilute regions, and the two cell types tend to be more segregated. When this option of ‘clustering’ is chosen, cells are only drawn if they are within a certain distance  $r_{cluster}$  of the nearest neighbor of the same species. Similar to the option of aligning rod-shaped cells, this clustering method only works after some cells are already present, so the creation of these images is performed in multiple steps. As before, a K-D tree is created for each species to determine nearest neighbor distances.

Together, these methods enable the creation of diverse synthetic images with rod-shaped and circular cells that are either clustered or randomly distributed and, in the case of

rods, randomly oriented or aligned to varying degrees. A set of sample images created with different input parameters is shown in Fig. S2. These images thus provide excellent training data for segmentation models suitable to different systems and imaging techniques. The extension of this approach to objects with other shapes only requires the creation of functions to draw those shapes.

## S2. SEGMENTATION MODEL TRAINING PARAMETERS

Within the Omnipose command line interface (CLI), the training command used to train the model for segmentation of monolayers of *Pseudomonas aeruginosa* (*P. a.*) was

```
omnipose --train --use_gpu --dir <image_folder_path> --mask_filter
_masks --n_epochs 2000 --pretrained_model None --learning_rate 0.1
--diameter 0 --batch_size 16 --RAdam --omni --nclasses 3 --tyx 224,224
--save_every 100 --save_each --verbose
```

In general, it is not guaranteed that the model trained at the last epoch produces the best segmentation results, so the model was saved at regular intervals to evaluate performance.

For all models trained to segment bacteria in mixed colonies of *P. a.* and *S. a.* (either in confocal or brightfield microscopy images), the training command used was

```
omnipose --train --use_gpu --dir <image_folder_path> --mask_filter
_masks --n_epochs 2000 --pretrained_model None --learning_rate 0.1
--diameter 0 --batch_size 16 --RAdam --omni --nclasses 3 --tyx 128,128
--save_every 100 --save_each --verbose
```

In all cases, the training converged quickly enough that no significant improvements could be obtained after 2000 epochs, and in some cases the best performance was obtained for models from earlier epochs. The difference in the parameter `--tyx` between the two commands is due to the difference in the size of the images in the training sets, as described in the main text.

### S3. CYCLEGAN TRAINING

As done in Ref. [1], we use discriminators for the microscopy images as well as for their Fourier transforms. For the real-space discriminators  $D_{X,\text{img}}$ , and  $D_{Y,\text{img}}$ , the loss functions are given with respect to the generators  $G : X \rightarrow Y$  and  $F : Y \rightarrow X$ :

$$\mathcal{L}[D_{X,\text{img}}] = \frac{1}{|\mathcal{D}_y|} \sum_{y \in \mathcal{D}_y} \|D_{X,\text{img}}(F(y))\|_2 + \frac{1}{|\mathcal{D}_x|} \sum_{x \in \mathcal{D}_x} \|1 - D_{X,\text{img}}(x)\|_2, \quad (3)$$

$$\mathcal{L}[D_{Y,\text{img}}] = \frac{1}{|\mathcal{D}_x|} \sum_{x \in \mathcal{D}_x} \|D_{Y,\text{img}}(G(x))\|_2 + \frac{1}{|\mathcal{D}_y|} \sum_{y \in \mathcal{D}_y} \|1 - D_{Y,\text{img}}(y)\|_2 \quad (4)$$

and similarly for Fourier-space discriminators  $D_{X,\text{FFT}}$ , and  $D_{Y,\text{FFT}}$ . Here  $\mathcal{D}_x$  and  $\mathcal{D}_y$  are the datasets for the real and simulated microscopy images, respectively, and  $\|\cdot\|_2$  is the L2 norm operator. For the generators, the loss functions are

$$\mathcal{L}[G] = \mathcal{L}_{\text{adv}}[G] + \lambda_{\text{cyc}} \mathcal{L}_{\text{cyc}}[F, G] + \lambda_{\text{id}} \mathcal{L}_{\text{id}}[G] \quad (5)$$

$$\mathcal{L}[F] = \mathcal{L}_{\text{adv}}[F] + \lambda_{\text{cyc}} \mathcal{L}_{\text{cyc}}[F, G] + \lambda_{\text{id}} \mathcal{L}_{\text{id}}[F] \quad (6)$$

Here, the adversarial loss  $\mathcal{L}_{\text{adv}}$  is the term that aims to fool its respective discriminator(s):

$$\mathcal{L}_{\text{adv}}[G] = \frac{1}{|\mathcal{D}_x|} \sum_{x \in \mathcal{D}_x} \|1 - D_{Y,\text{img}}(G(x))\|_2 + \frac{1}{|\mathcal{D}_x|} \sum_{x \in \mathcal{D}_x} \|1 - D_{Y,\text{FFT}}(G(x))\|_2 \quad (7)$$

The cycle-consistency loss is given by

$$\mathcal{L}_{\text{cyc}}(F, G) = \frac{1}{|\mathcal{D}_x|} \sum_{x \in \mathcal{D}_x} \|F(G(x)) - x\|_1 + \frac{1}{|\mathcal{D}_y|} \sum_{y \in \mathcal{D}_y} \|G(F(y)) - y\|_1 \quad (8)$$

and the identity loss is given by

$$\mathcal{L}_{\text{id}}(G) = \frac{1}{|\mathcal{D}_y|} \sum_{y \in \mathcal{D}_y} \|G(y) - y\|_2. \quad (9)$$

For the cycle-consistency loss,  $\lambda_{\text{cyc}}$  was 10, and for the identity loss,  $\lambda_{\text{id}}$  was 5. Fig. S3 shows the loss functions of the discriminators and generators as a function of the epoch in training. All the models are constructed with Tensorflow and run locally. There, training a cycleGAN model from scratch takes around 8 hours to complete using a single NVIDIA 3090 GPU.



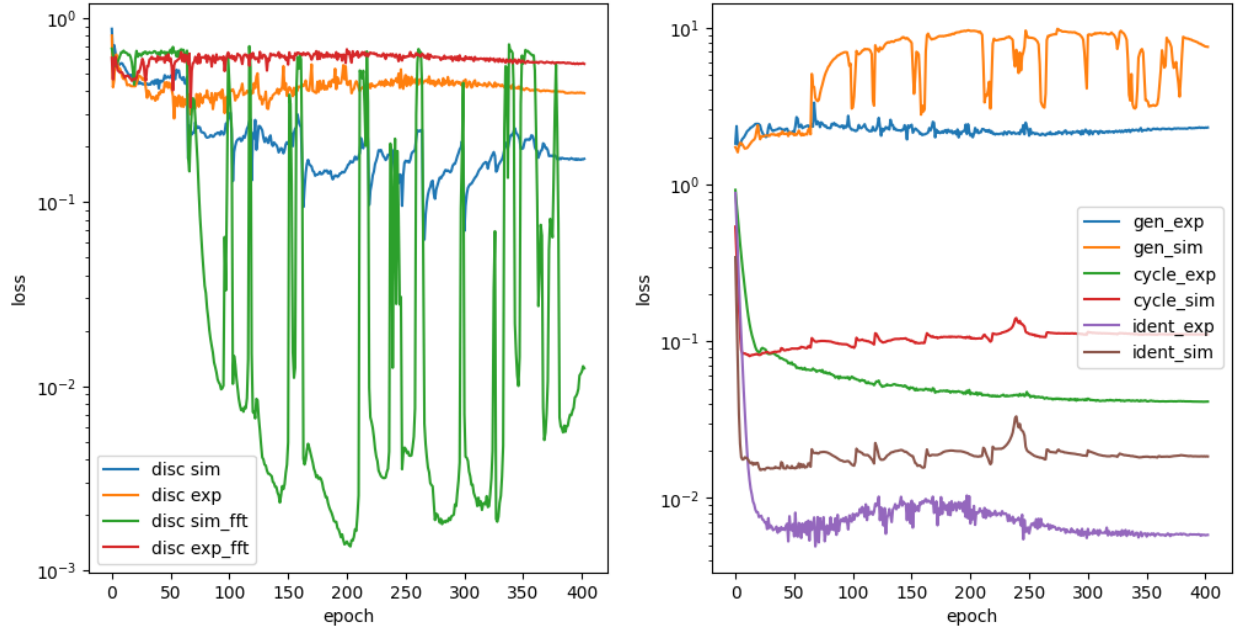


FIG. S3. Losses of the discriminators (left) and the generators (right) vs training epoch.

- 
- [1] Abid Khan, Chia Hao Lee, Pinshane Y. Huang, and Bryan K. Clark. Leveraging generative adversarial networks to create realistic scanning transmission electron microscopy images. *npj Computational Materials*, 9(1):1–9, May 2023. ISSN 2057-3960. doi:10.1038/s41524-023-01042-3. URL <https://www.nature.com/articles/s41524-023-01042-3>.